Fault Detection and Diagnosis for Indoor Air Quality in DCV systems: Application of 4S3F method and effects of DBN probabilities.

Arie Taal[a] ,Laure Itard[b]

[a] Department of Mechanical Engineering, The Hague University of Applied Sciences, Delft, The Netherlands
[b] Research Institute OTB, Delft University of Technology, Delft, The Netherlands

Abstract

In this article a generic fault detection and diagnosis (FDD) method for demand controlled ventilation (DCV) systems is presented. By automated fault detection both indoor air quality (IAQ) and energy performance are strongly increased. This method is derived from a reference architecture based on a network with 3 generic types of faults (component, control and model faults) and 4 generic types of symptoms (balance, energy performance, operational state and additional symptoms). This 4S3F architecture, originally set up for energy performance diagnosis of thermal energy plants is applied on the control of IAQ by variable air volume (VAV) systems. The proposed method, using diagnosis Bayesian networks (DBNs), overcomes problems encountered in current FDD methods for VAV systems, problems which inhibits in practice their wide application. Unambiguous fault diagnosis stays difficult, most methods are very system specific, and finally, methods are implemented at a very late stage, while an implementation during the design of the HVAC system and its control is needed. The IAQ 4S3F method, which solves these problems, is demonstrated for a common VAV system with demand controlled ventilation in an office with the use of a whole year hourly historic Building Management System (BMS) data and showed it applicability successfully. Next to this, the influence of prior and conditional probabilities on the diagnosis is studied.

Keywords: 4S3F framework; Fault Detection and Diagnose (FDD); Demand controlled ventilation (DCV); Diagnostic Bayesians Networks (DBN); Building management Systems (BMS); Energy Performance; Indoor Air Quality (IAQ)

Abbreviations

AHU	Air handling unit
BMS	Building management system
DBN	Diagnostic Bayesian network
DCV	Demand controlled ventilation
EP	Energy performance
EWMA	Exponential weighted moving averages
F	Fault
FDD	Fault detection and diagnosis
HVAC	heating, ventilation and air conditioning
IAQ	Indoor air quality
OS	Operational state
PCA	Principle component analysis
PIR	Passive infrared
P&ID	Piping & Instrumentation Diagram
S	Symptom
THUAS	The Hague University of Applied Sciences
VAV	Variable air volume
4S3F	4 faults and 3 symptoms

Symbols

CO2	CO_2 concentration [ppm]
q_V	Volume flow rate [m3/h]
PIR	presence [0,1]
P	Probability [0..100 %]

1. Introduction

Demand Controlled Ventilation (DCV) is claimed to be an effective method to achieve both high indoor air quality (IAQ) and energy savings. It determines the air flowrate to rooms according to the actual requirements in air-conditioned zones based on CO_2 concentration (see e.g. Fisk et al. [1] who presented an overview of DCV systems and ASHRAE standard 62.1 2013[2]). Most of the time the air flow rates are reduced significantly by DCV compared with conventional ventilation methods. In this article we focus on DCV systems controlling CO_2 concentration in workspaces.

The benefits of DCV in comparison with constant air-volume systems are the reduction in heating and cooling load of the supply air and the decrease in power consumption of air handling unit (AHU) fans. Studies showed up to 40 % energy savings for fans. Tukur et al. [3] noted 25 % for an office building, Nielsen et al. [4] 35 % for family houses and Schibuola et al. [5] 40 % for a library. Zhang et al. [6] found energy savings for fans between 12 and 30 % for 15 locations in the United States. Thermal energy savings up to 25 % are depicted in [6].

Despite these positive results, generally in practice, the expected energy savings are not always realized. From a survey by Qin et al. [7] it followed that 20,9 % of the considered VAV terminals were ineffective, leading to poor IAQ and energy performance (see Lee and Yik [8], Wang [9], Guo et al. [10], who showed energy waste up to 30% for air systems, and Yu et al. [11] with energy waste between 25 and 50%). Many causes were identified in design, realization and operational stages, like faulty capacities of components, incorrect control of the DCV system or faulty sensors, see for instance Okochi and Yao [12], who stated that VAV systems can still be improved because faulty CO_2 and occupancy sensors are common due to aging and incorrect sensor placement in rooms. Additionally, needed air ventilation capacities may have not been installed because of poor design or implementation.

Moreover, CO_2 is used as proxy for indoor air quality and incorrect control of the indoor quality leads to health and comfort problems. Thus, neither energy savings or indoor quality are guaranteed.

Various types of DCV methods are available, such as occupancy presence control, relative humidity control and CO_2 control, see e.g. [13 and 14] and temperature control in VAV systems. CO_2-based DCV controlled method is most commonly used and we focus on it in this article.

Although CO_2 sensors could be placed in the rooms or in the room return air ducts, they are often installed in the main return air duct to limit costs. For instance, Shan et al. [9] proposed a multi-zone demand-controlled ventilation strategy using a limited number of CO_2 sensors in the main return air duct. However, nowadays the increased requirements for smart buildings, combined with the decrease of CO_2 sensor prices result in buildings being equipped with CO_2 and occupancy sensors in workspace. In these smart environments, DCV is controlled by both CO_2 concentration and occupancy. Many control strategies are available. Okochi et al. [12] presented an overview of controllers for VAV systems. Chenari et al. [14] presented also an overview of ventilation strategies. Conventional controllers are encountered (like P, PI PID) and predictive and adaptive controllers. For instance Lu et al. [15] presented a dynamic DCV strategy using CO_2 balances equations, Goyal et al. [16] discussed the control of occupancy-based zone-climate, See also control strategies by Chao and Hu [17] and Wang [18] .

More complex control systems lead to more chance of faults, meaning that the use of FDD (Fault detection and diagnosis) methods has become inevitable. Correction of the diagnosed faults will lead to better indoor air quality and lower energy consumption of fans and heating and cooling coils in the air handling units.

Kim and Katipamula [19] have presented recently an overview of FDD methods for HVAC systems including VAV systems. See for instance [7, 20 and 21] for VAV terminal units, Schein et al. [22] presented a method called VPACC (VAV box performance assessment control charts). FDD for the whole VAV systems is also available, see e.g. [23]. Most of the methods for VAV systems are based on expert rules [24] and can be combined with an approach with control charts using e.g. cumulative sum [24] and exponential weighted moving averages (EWMAs) [22] to eliminate transient influences and incidental outliers by measurements. In [7, 22 and 24] lists of faults and symptoms in VAV end-terminal systems are presented. Unfortunately, they are specific to the kind of considered system and generic FDD methods are still missing.

In the last decade data-driven methods were popular. Du and Jin [25] applied a principle component analysis (PCA) method to determine sensor faults and to correct them. Qi and Dong [26] proposed a FDD model for VAV systems based on neural networks. An issue here is that data-driven FDD methods use energy data based on sensors that may be faulty, and on heating, ventilation, air conditioning (HVAC) operation mode which is not always known. A novel approach is the use of Bayesian statistics. Xiao et al. [27] presented a diagnostic Bayesian network (DBN) for FDD of VAV terminals. Regnier et al. [28] proposes to apply it on AHU and VAV while Zhao et al. [29 to 31] applied DBN on AHU and chiller faults. Verbert et al. [32] also applied DBN on HVAC systems and Chen et al. [33] on whole building.

However, in all these FDD approaches the implementation does not occur simultaneously with the design of the HVAC system and its control. In [34], it was shown that the fact that FDD design does not take place concurrently with the design of HVAC and its control system, is a reason for the lack of use of FDD. The implementation of available FDD methods is complicated because it is time-consuming and their structures deviate from HVAC design or control engineer practice.

In this article we apply the 4S3F framework which integrates these methods into an FDD architecture that can be set up by HVAC and control engineers during the design process, and is based on Piping & Instrumentation Diagrams (P&IDs).

In [34] we have proposed a generic architecture for Energy Performance (EP) FDD, the so-called 4S3F method based on DBNs which can be setup simultaneously with HVAC design and implementation. This approach is based on HVAC P&IDs.

The advantages of the DBN approach as stated in [34] are:

- It is congruent to HVAC design and implementation practices.
- Fault identification takes place simultaneously at different system levels which prevent a complex top down or bottom up FDD approach.
- Outcomes are probabilities as an HVAC expert diagnoses.
- It delivers results even when information is missing or contradictory.
- It allows the application of all kinds of FDD methods to estimate or exclude symptoms and faults.

The examples in [34] are based on thermal energy plants in buildings. Here, we propose to apply it to DCV systems.

Section 2 introduces the 4S3F method and in section 3 the DCV system is explained. In sections 4 to 8 the DCV 4S3F method is applied in a case study for a lecturer room of a school building. Section 4 describes the 4S3F model in the case study. Then the results of the IAQ diagnosis are discussed. First, in section 5 basis analysis with the help of performance graphs is addressed from hourly available building management system (BMS) data. Then, in section 6 symptom results are shown from automated detection and finally the estimated faults are derived by applying diagnosis by a DBN model based on the 4S3F architecture in section 7. In section 8, the results are evaluated and in section 9 sensitivity of prior and conditional probabilities with regard to diagnosis results are discussed. Finally, conclusions are drawn from the case study and recommendations for further research are proposed in section 10.

2. The 4S3F FDD method for indoor air quality.

The reference EP FDD architecture described in [34] consists of four generic types of symptoms (4S): balance, energy performance (EP), operational state (OS) and additional symptoms. A balance symptom is present when a deviation in an energy, mass or pressure balance for a system is detected. When an energy performance metric, like a performance factor (e.g. coefficient of performance COP) or energy use shows a too low value an EP symptom is found while when a state value (e.g. temperature, flow rate, pressure, on-off state of a component) deviates unexpectedly in time, an OS (Operational State) symptom is detected. These state values could be measured by the BMS and are mostly depicted in an HVAC P&ID. Additional symptoms based on for instance inspection or maintenance information, or from specific FDD methods of HVAC components can be added if needed. We recall that a symptom must be observable (is therefore the result of measurements) and symptoms can be identified by listing all measurement points (sensors) in the P&ID while a fault is the system 'disease' that leads to symptoms. Possible faults can be listed on the same way by observing the P&ID.

Three generic types of faults (3F), model, component and control faults, are present. The first ones are faults in assumptions in the models estimating values for missing data. The second relates to HVAC components and systems which do not function properly. For instance too low installed capacity, or too low efficiency by aging, or because it is defect. The last type concerns faults in the control of the HVAC components and system, for instance control of supply temperatures and on-off strategy of components like the control of the sequence of energy generators. Fig. 2.1 shows relations between fault and symptom types in this 4 symptom and 3 faults (4S3F) method. For instance, a component fault could lead to balance, EP, OS and additional symptoms. In contrary, an EP symptom could be caused by a model, component or control fault. As can be seen there is no univocal relationship between faults and symptoms because more faults can lead to a same symptom. See [34] where this is explained in more detail.

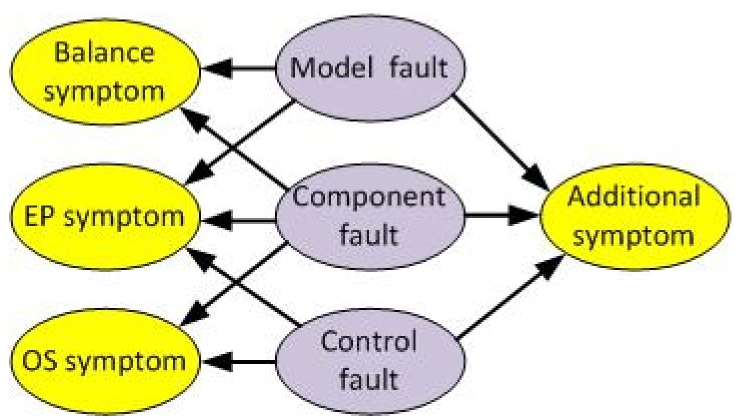

Fig. 2.1 The 4S3F model: Relations between fault and symptom types.

With the help of a diagnostic Bayesian network (DBN) model, diagnosis takes place simultaneously in all components and systems. The DBN model of the 4S3F consists of the fault nodes which are linked to the symptoms nodes as shown in Fig. 2.1. The fault nodes are so-called parent nodes with prior probabilities for their states and the symptom nodes are so-called child nodes with conditional probabilities for their states depending on the state of the fault nodes. The probabilities of the fault states, a value between 0 and 1, are calculated by the DBN when the states of the symptoms are known.

In this paper the 4S3F model developed for energy performance diagnosis is extended to DCV. This reference architecture supports all kind of DCV systems controlling CO_2 concentration at room level and is demonstrated on a quite common DCV system, see Fig. 3.1.

3. Faults and symptoms of demand controlled air ventilation systems

In this section generic faults and symptoms for DCV systems are identified and analyzed. Fig. 3.1 shows a P&ID, as used during design, of a frequently applied DCV system in which the supplied air flow rate is controlled by room dampers placed in end-terminals. The damper position depends on the presence of people and CO_2 concentration in the room. The air flow to the room is controlled by the CO_2 controller (CC) and the CO_2 concentration measured by the concentration transmitter (CT).

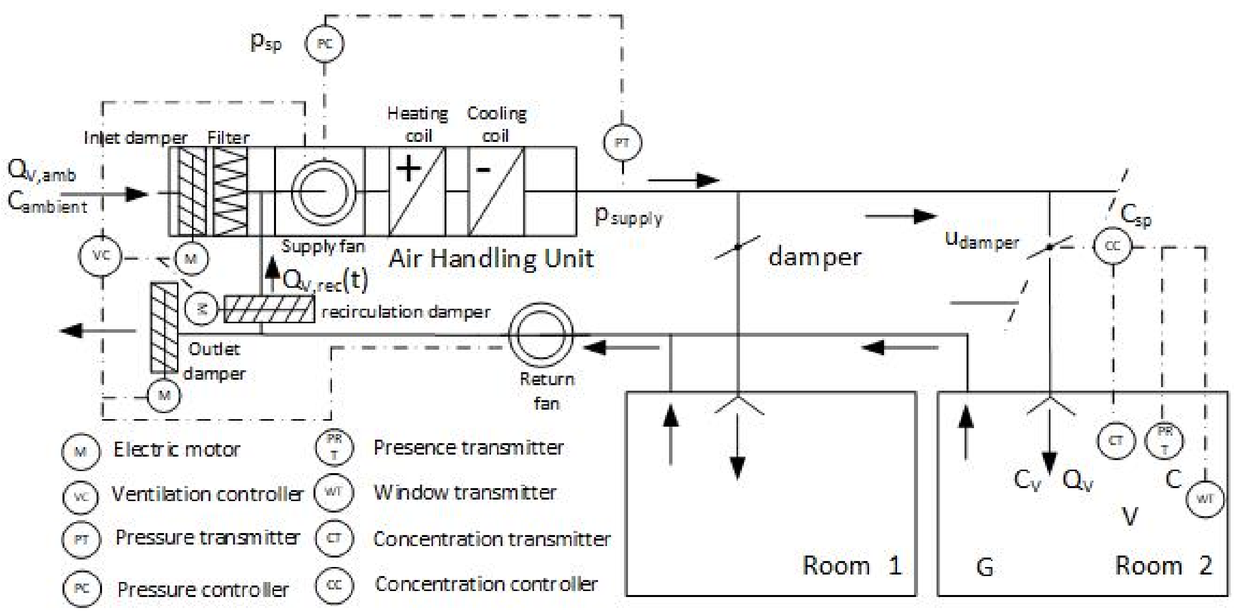

Fig. 3.1 P&ID of a VAV system

G=CO_2 production in the room [kg/s].

C=CO_2 concentration in the room [ppm].

C_{sp}=setpoint of the maximum CO_2 concentration in the room [ppm].

p_{sp}=setpoint of static pressure of the supply air [Pa].

p_{supply}= Static pressure of the supply air [Pa].

C_v=CO_2 concentration of the supply air [ppm].

$C_{ambient}$=CO_2 concentration of ambient air [ppm].

$Q_{v,ambient}$=ambient air rate flow [m^3/s].

Q_v=supply air rate flow to the room [m^3/s].

$Q_{v,rec}$=recirculated air flow rate [m^3/s].

u_{damper}= damper position [0..100 %].

V=room air volume [m^3].

The fresh air to the rooms is supplied by the supply fan which is located in the Air Handling Unit. When room dampers are closed or partly opened, the supply and return fans in the AHU have to deliver less air flow. Usually, this can be controlled by a pressure controller (PC) which regulates the rotation speed of the fans. In the supply duct after the AHU the controlled supply pressure is measured by a pressure transmitter (PT). Controller VC opens and closes the inlet, recirculation and outlet dampers of the AHU and set the supply and return fans on and off by timers and ventilation demand.

There are also adapted versions of these control strategy (like Fig. 3.1), at room level where also the presence of people (measured by a sensor indicated as PRT) and opened windows (measured by WT) are taken into account, as well as system level where the needed supply air flows are calculated by occupancy and CO_2 levels in the rooms. In the specific case study (see section 4), the mechanical ventilation is shut down to avoid energy losses when the windows are open. It is very easy, using the P&ID in Fig. 3.1, to list all possible symptoms and faults. This is done in Appendix A and forms the basis for the 4S3F architecture.

4. 4S3F model for DCV systems in a case study

In this section the application of the 4S3F model to a real DCV system is shown. In the school building of The Hague University of Applied Science (THUAS) in the Netherlands a demand driven air ventilation system is present in which the air flow to the rooms is controlled by CO_2 concentration and occupancy.

The case study has been conducted on historical data of a room of the THUAS building. Hourly BMS data is available for the year 2015 and we will conduct diagnosis on hourly basis which can also be done on actual BMS data. The location of this room 1.067, a lecturer room, is shown in Fig. 4.1. In an occupied room, the air flow rate is increased when the CO_2 concentration exceeds 800 ppm and is decreased when it is below 600 ppm and the room is unoccupied. The designed supply air flow rate is 200 m^3/h based on presence of 4 persons.

Most rooms of THUAS are located to an outer wall and contain windows. In each room of the building under consideration the CO_2 concentration is controlled by a damper which is present in the supply air duct to the room. A very specific control feature is that when one of the windows in the room is opened the mechanical air supply is stopped. This is to avoid energy losses. The presence is measured by a (passive infrared) PIR sensor and at the windows magnetic contacts are present which indicate an opened window. The supply air rate to a room is restricted by design and implementation of specific dampers with fixed maximum air flow rate setting. The air leaves the rooms by overflow to the corridors where return vents are present.

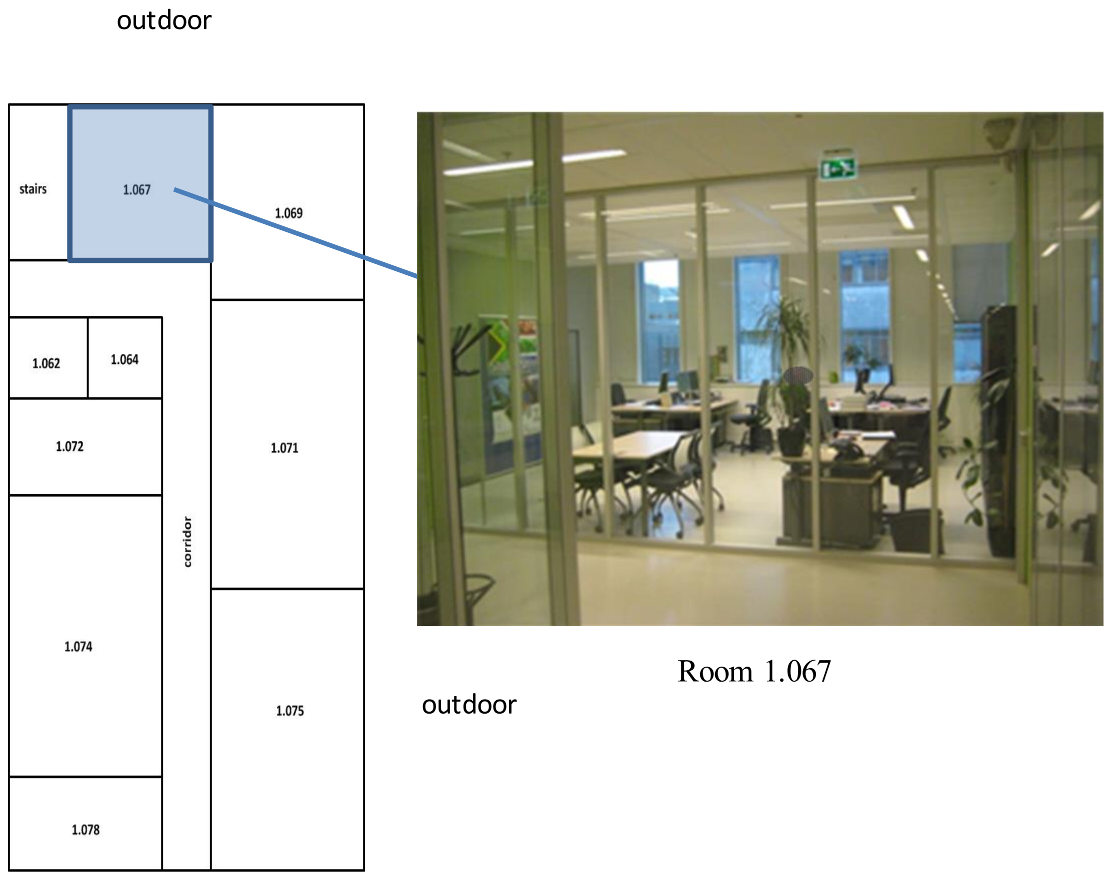

Fig. 4.1 Considered building section

Too high measured CO_2 concentration in a room, one of the OS symptoms, could have, if present, many causes: by a faulty CO_2 sensor (e.g. broken), a faulty CO_2 measurement (e.g. biased value), missing connection to the BMS, a supply fan of the AHU which is not running, an occupancy sensor which is stuck, an occupancy measurement value is frozen, the damper of the VAV system which is broken or the control of it which is frozen. See Table 3.1. But also by occupancy behaviour: the room occupancy can be higher than intended and in case of THUAS, one or more windows can be opened which leads to close the damper in order to save energy.

4.1 Considered faults in the case study

The faults in this case study are based on the generic faults presented in Appendix A in which faults are coded from F1 to F19. As simplification we do not look at the cause inside a component and cluster all faults concerning one component for the sake of demonstration. So a broken or biased CO_2 sensor are clustered to one fault for the component CO_2 sensor, namely a faulty CO_2 sensor (F8). In addition faults due to the AHU like damper (F4), filter (F5) and fan (F3) faults, and faults to control the AHU (F14, F15 and F17) are clustered to one component fault for the AHU because with the available BMS data in the case study it is not possible to distinguish the faults inside the AHU. However, when control values of the fan and dampers are present in the BMS, they could be separated. We have also clustered faults concerning the room damper (F7). A correct measured mechanical flow is important to detect symptoms. That is why we also take into account the air flow sensor qV as a fault (F11).

Table 4.1 presents the 9 faults which are considered in the case study. As can be seen 6 components and 3 control faults (CO2, window and occupancy control) are distinguished. Three components are sensors: CO_2, PIR and qV sensors. Except fault F19, window control, which is specific for the THUAS building, all faults are generic for DCV systems with room control.

As can be seen model faults F1 to F2 are not taken into account in the case study because virtual sensors were not applied. Furthermore, air leakage of ducts (F6) is ignored.

FAULTS				SYMPTOMS			
Nr	**Description**	**Type**	**Explanation**	**Nr**	**Description**	**Type**	**Rules and thresholds**
1	*Occupancy*	Control	The occupancy in the room is higher than according to the requirements.	**h**	*High CO2 and high qV*	OS	CO2>840 ppm and qV>200 m3/h PIR=1
2	*CO2 sensor*	Component	It can be broken or biased, or a cable is not connected or broken.	**a** **b** **j**	*CO2 unrealistic* *CO2 missing* *ΔCO2 neighbours*	OS OS Balance	CO2<360 or CO2>3000 ppm CO2=NaN |ΔCO2 other rooms|/CO2 on Saturdays from 0:00 to 6:00 am.
3	*AHU*	Component	It can be broken or the control of it is not right.	**g** **m** **i**	*qV_AHU=0* *qV=0* *High CO2 and qV=0*	OS OS OS	qV_fan=0 and PIR=1 qV=0, PIR=1and Δt=6 hrs. CO2>840 ppm, qV=0 m3/h and PIR=0
4	*PIR sensor*	Component	It can be broken or biased, or a cable is not connected or broken.	**c** **d**	*ΔCO2 and PIR=0* *Presence outside working hours*	Balance OS	ΔCO2>40 ppm. PIR=0 and Δt=1 hr. PIR=1 and 0:00<t<6:00 am
5	*Damper*	Component	The mechanical part of the damper or the electrical motor is stuck.	**i** **k** **l** **m**	*High CO2 and qV=0* *High CO2 and low qV* *Low CO2 and qV>0* *qV=0*	OS OS OS OS	CO2>840 ppm, qV=0 m3/h and PIR=0 CO2>840 ppm, 0<qV<100 m3/h and PIR=0 CO2<500 ppm, qV>0 m3/h and Δt=5 hrs. qV=0, PIR=1and Δt=6 hrs.
6	*qV sensor*	Component	It can be broken, or a cable is not connected or broken.	**e** **f**	*qV unrealistic* *qV missing*	OS	qV>400 m3/h or qV<0 m3/h. qV=NaN
7	*BMS*	Component	A broken data-connection or software failure in the data logging leads to missing data.	**f** **b**	*qV missing* *CO2 missing*	OS	qV=NaN
8	*Window control*	Control	The air supply to the room is stopped when a window is opened.	**i**	*High CO2 and qV=0*	OS	CO2>840 ppm, qV=0 m3/h and PIR=0
9	*CO2 control*	Control	The CO2 setpoints are not correct: too high at occupancy or too high at un-occupancy. Or delay times are too long.	**k**	*High CO2 and low qV*	OS	CO2>840 ppm, 0<qV<100 m3/h and PIR=0

Table 4.1 Overview of faults and corresponding symptoms in the case study (we have renumbered the faults and symptoms in Table A.1)

4.2 Considered symptoms in the case study

Table 4.1 also presents the 13 symptoms (depicted as **a** to **m** and based on the symptoms S1 to S13 presented in Appendix A,) that would be the observable result of the 9 faults identified in section 4.1. Except for the balance symptoms, all symptoms are OS symptoms, meaning that the operational performance is compared to preset values. These preset values can be control setpoints and also expert rules. This approach is generic, but evidently, the setpoint values are DCV system specific.

Symptom *CO2 unrealistic* (type S8 in Table A.1, type **a** in Table 4.1) is present when the measured CO_2 value is lower than the outdoor value or higher than an extreme value which indicates a non-realistic CO_2 measurement. When the BMS has not stored a CO_2 or a qV measurement, the value is not-a-number (NaN) which leads to symptom *CO2 missing* or *qV missing* (both type S7, **b** and **f**). Symptom *qV unrealistic* indicates a negative value or a much higher value than should be possible on the basis of the design specifications (type S8, **e**). *High CO2 and high qV* (type S4, **h**) represents that CO_2 is higher than the desired value with maximum air rate flow at room occupancy. In the same way *High CO2 and qV=0* and *High CO2 and low qV* (also both type S4, **i** and **k**) indicates too high CO_2 at absence or low value of the air flow rate to the room. During the weekends, when the building is unoccupied, the CO_2 values in rooms located close to each other should decrease to the same level. Symptom *ΔCO2 neighbours* (type S1, **j**) is present when the CO2 concentration the room deviates 10 % from the mean value of the adjacent rooms at the end of Sunday night. When the CO_2 level is acceptable while an air flow rate is present, the symptom *Low CO2 and qV>0* (type S5, **l**) is present because ventilation should not be needed. Symptom *qV_AHU=0* (type S6, **g**) is observable when the air handling unit does not supply air while the room is occupied. A room occupancy measured during night or weekend time also indicates the symptom *Presence outside working hours* (type S9, **d**). It could not be possible that the CO2 concentration increases in the room while the PIR sensor indicates unoccupancy. Then symptom $\Delta CO2$ *and PIR=0* (type S1, **c**) is present. At last, when symptom *qV=0* (type S6, **m**) is observable when the room is occupied while ventilation is not present.

Notice that symptoms **c**, **h**, **i**, **k** and **m** are formed from combinations of measurements. To eliminate transient influences sufficient time periods should be taken into account.

As depicted in Table 4.1, some symptoms are only detected when they are present during more than one hour to avoid faulty detection by transient behaviour and incidental measurement outliers.

The chosen values in the rules are building specific and depend on the outdoor condition, the designed HVAC system and the HVAC control set points. The purpose of this article is not to optimize them, we have chosen values which obviously could be different in other systems. They are presented in the last column.

4.3 DBN model in the case study

In the 4S3F DBN method Bayesian statistics is applied which is based on relations between state probabilities of events. When the probability that event B is true (P(B)=1), the conditional probability P(A|B) that event A occurs while B is true, can be estimated using the DBN model. See Appendix B in which this is explained. In the DCV DBN events are faults which are linked to events for symptoms by arcs. When the true and false states of the symptoms are known, the posterior state (true or false) probabilities can be estimated.

Table 4.1 shows the links between the faults and symptoms in the DCV DBN model.

This table is implemented straight forward in a DBN model. See Fig. 4.2.

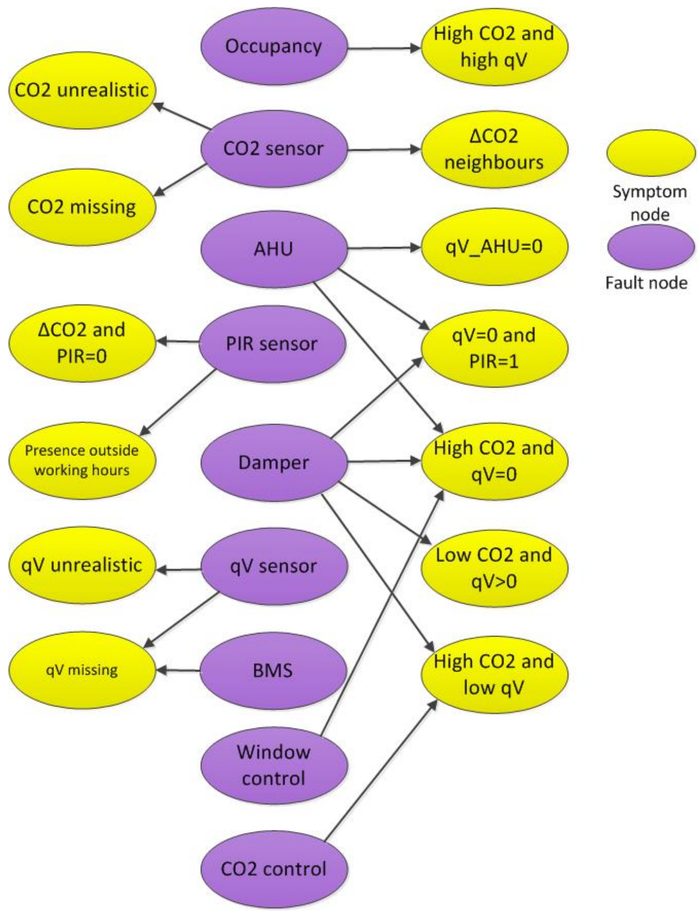

Fig. 4.2 DBN model of DCV system in the case study (faults in purple, symptoms in yellow).

Set probabilities in the DCV DBN model

The values of the prior and conditional probabilities in the DCV DBN are based on assumptions. In the DCV DBN mode, the fault nodes (purple color) are parent nodes having prior probabilities which are set between 90 and 99 % true value. Thus it is taken into account that some faults happen more often than others. For instance, a damper (1 % probability it is defect, see Appendix B) is seldom stuck while an opened window (5 % probability, see Appendix B) is more common. The symptom nodes (yellow color) have conditional probabilities which values indicates the probabilities that the symptom is present or absent depending on the state of the parent nodes. As example we take symptom high CO2 and no qV which can be caused by a disabled supply fan (AHU fault), by a frozen closed damper (Damper fault) or by opened windows (wrong Window control). The disabled supply fan leads with high probability (70 %, see Appendix B) to this symptom. This value is lower than 100 % because an opened window could deliver enough ventilation which does not lead to detection of the considered symptom. Another example is that an incorrect damper can be closed or opened. Only a frozen closed damper does not lead to mechanical ventilation. We assume that the probability of a frozen closed damper is as large as a frozen opened damper which lead to a conditional symptom probability of 50 % (see Appendix B) when the damper is faulty. And at last the example that windows are opened, thus mechanical ventilation is stopped. However, this will not always lead to high CO_2 concentration because the natural ventilation can be sufficient. So we have assumed a conditional probability of 40 % that a opened window leads to too high CO_2 concentration.

Diagnosis can present fault probabilities in percentages. The absolute value is less important than the relative value. For instance, a diagnosed fault probability between 30 and 100 % should lead to analyze the fault. We propose to look at the highest fault probabilities, e.g. higher than 30 % and start with the highest one for analysis purposes as an expert would do.

5. Monitoring results and descriptive analysis of BMS data

As background information, we address in this section first the measurements as energy signatures without using our 4S3F method for year 2015. Fig. 5.1 shows the measured CO_2 concentration in the rooms 1.067, 1.069, 1.071 and 1.075 (the location was shown in Fig. 4.1) during the year. Notice that weeks and days can be distinguished by peaks and valleys of the CO_2 levels and that they are low during end July and begin August (around 400 ppm) corresponding to an empty building during summertime. Furthermore, at the begin of the year the CO2 concentration is higher, more than 2000 ppm!) than in the rest of the year. In most cases the CO_2 concentration stays below 1500 ppm.

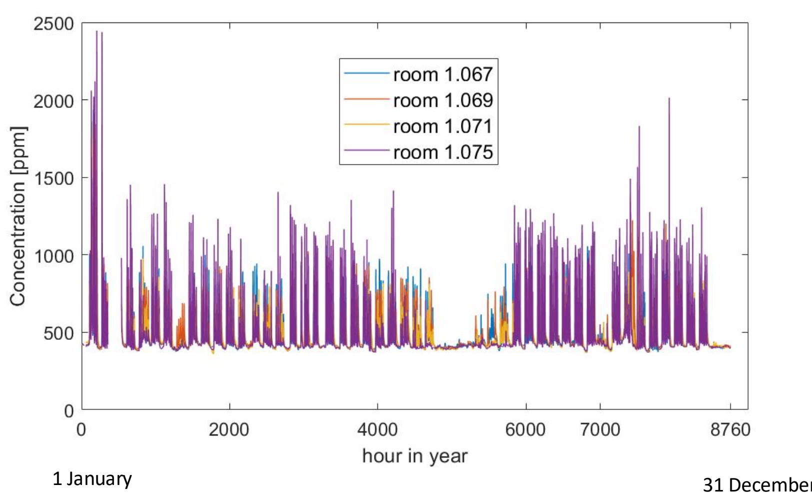

Fig. 5.1 CO_2 concentrations in room 1.067, 1.069, 1.071 and 1.075

Fig. 5.2 shows the time series plot for the mechanical air flow rate to room 1.067.

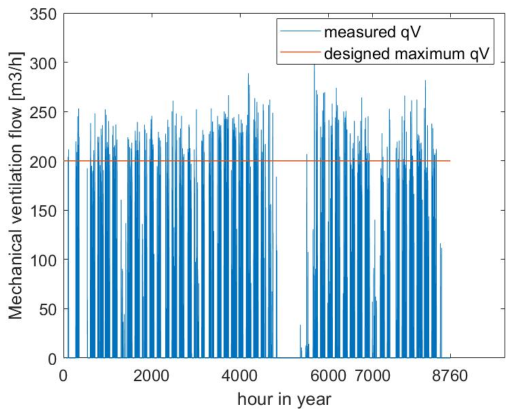

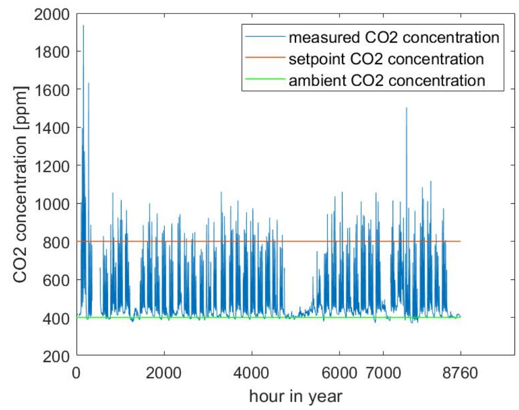

Fig. 5.2 Air flow rate to room 1067

Fig. 5.3 CO_2 concentration in room 1067

We see that the maximum air flow rate stays under 250 m^3/h most of the time, which is higher than the designed value of 200 m^3/h. Next we see that during summer ventilation was off. Furthermore we see a week pattern. Fig. 5.3 depicts the CO_2 concentration of room 1067. The CO_2 concentration is around 800 ppm during room occupancy which is the set point value. Outliers are detected at the begin of the year and at the end of the autumn. The ambient concentration (400 ppm) is an assumption based on outdoor values in the Netherlands.

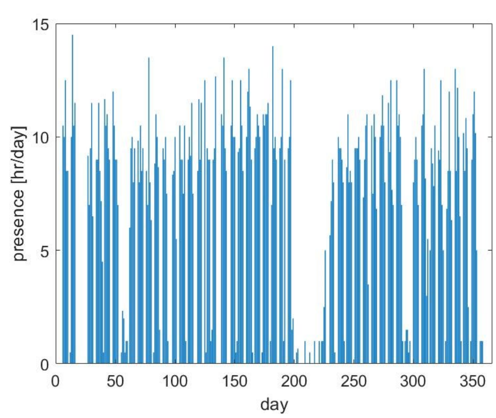

Fig. 5.4 Occupancy of room 1067

Fig. 5.4 depicts that the room is nearly unoccupied during summer time and at Christmas time.

In Fig. 5.5 we see that the building is occupied from Monday to Friday (weekdays 2 to 6). Fig. 5.6 shows that no air and a little bit of air was supplied on Sundays and Saturdays. The mean presence values are calculated by counting the hours that the room was occupied during a day. The daily mean air flow rates were calculated by summarize the measured air flow rate for all days and divide it by the daily period of 24 hour.

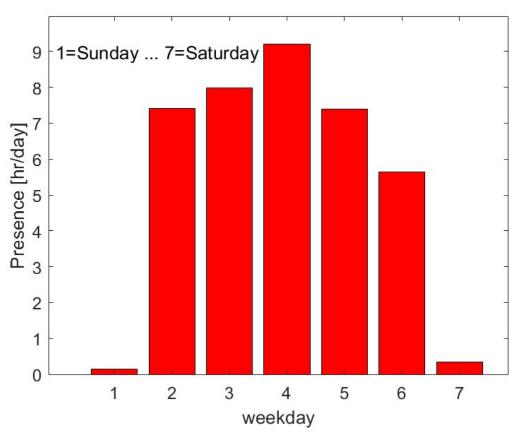

Fig. 5.5 Presence during weekdays

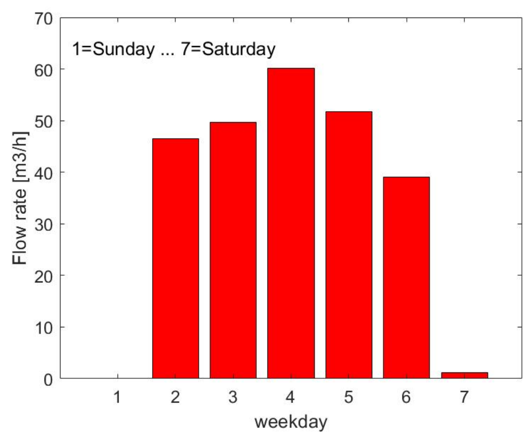

Fig. 5.6 Mean air flow rate during weekdays

From these signatures, the presence of symptoms, e.g. the high CO_2 values at the begin the year, is observed but does not lead to fault identification. It is almost impossible, also for the HVAC expert, to diagnose faults with these energy signatures or to optimize the system. Furthermore, symptoms can only be detected by outliers for which many (normal) data is needed and automation is not possible.

6. Application of the 4S3F method: Detected symptoms

In this paper, we used historical BMS data on the year 2015. They were uploaded in Matlab, in which the rules and setpoints of Table 4.1 were used to detect symptoms. In an automated building energy management they would be directly programmed into the BMS or could be an extension of the BMS. Fig. 6.1 (a) to (m) present the detection results for the 13 distinguished symptoms. In these figures the value 0 indicates that the symptom is present and a value 1 it is not.

Figs. 6.1 (a), 6.1 (b), 6.1 (e) and 6.1 (f) depict the detection results of symptoms **a**, **b**, **e** and **f** concerning the CO_2 and qV measurements. We see from these figures that the qV values and the CO_2 values are missing in some periods and that unrealistic values for these sensors are not present.

Figs. 6.1 (c) and 6.1 (d) are about the occupancy sensor. This figures show that these symptoms for the PIR sensor are missing.

Fig. 6.1 (h), 6.1 (i), 6.1 (k) and 6.1 (l) depict symptoms about CO_2 concentration and air ventilation flow. Fig. 6.1 (h) shows that '*high CO2 with high qV*' is present. Notice that this symptom is often present during June and September.

Symptoms i, k and l are shown in Fig. 6.1 (i), 6.1(k) and 6.1 (l). Symptom **l** is not present (ventilation while the CO_2 concentration is low) while the presence of symptoms **i** and **k** (thus high CO_2 while the ventilation is not present or low at occupancy) can be seen. Fig. 6.1 (j) depicts that symptom j (*ΔCO2 neighbours*) happened once. In Fig. 6.1 (g) we see that the supply fan is sometimes off while the room is occupied. Fig. 6.1 (m) shows that symptom m ($q_V=0$) is present only once.

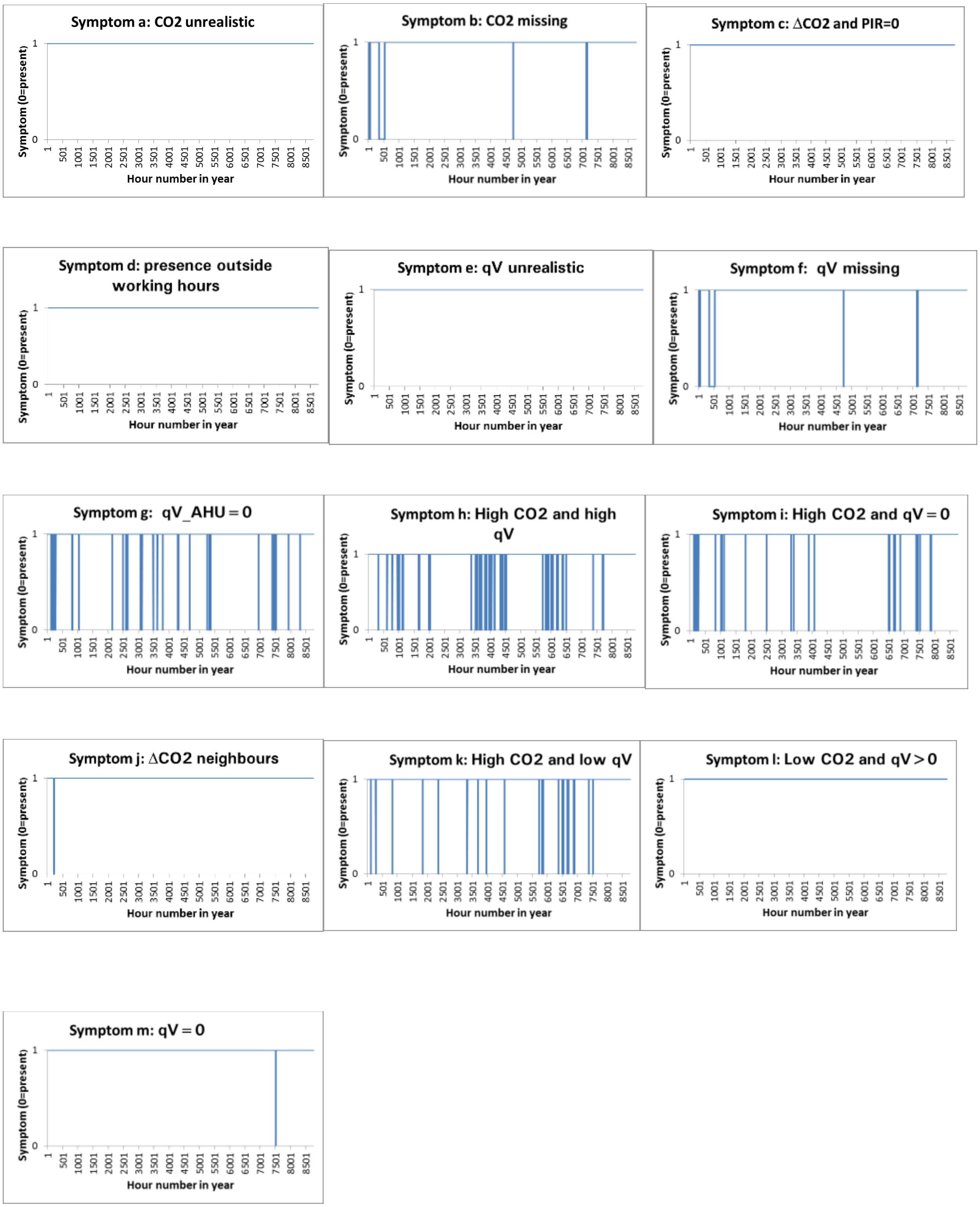

Fig. 6.1 Detected symptoms **a** to **m**

(0=present, 1 = absent; hour 1=1 January, hour 8760=31 December)

This automated symptom detection is an improvement compared to the application of energy signatures as mentioned in section 5 in the sense that detection is automated and that a clear list of symptoms is generated. However, it is still complicated to find out the faults leading to symptoms. For example, one might estimate that sensor errors are absent from symptoms **a** to **f**, but it is more difficult to interpret symptoms **g** to **i** and **k**.

7. Application of the 4S3F method: Diagnosis results

In this section faults are isolated automatically from detected symptoms. The scheme depicted in Fig. 4.1 is built in Genie. Then the absent and present symptoms detected in Fig. 6.1 are fed to the DBN. Diagnosis has taken place for each hour in 2015. The diagnosis results are presented in Fig. 7.1. The value 0 indicates that the fault is present and the value 1 it is not.

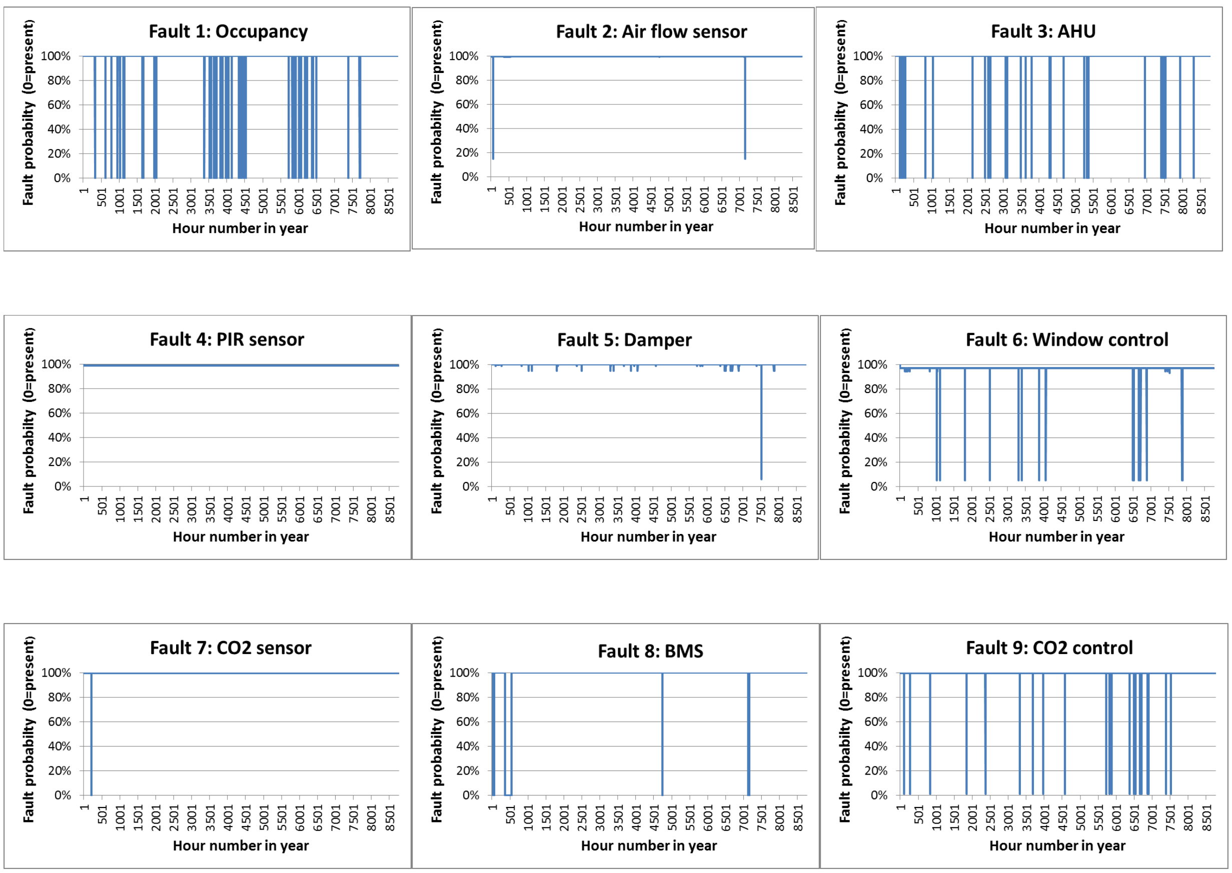

Fig. 7.1 Faults 1 to 9 (0=present, hour 1=1 January, hour 8760=31 December)

First we address sensor faults. Fig. 8.1 (4) shows that the PIR sensor is always correct. Figs. 7.1 (2) and (7) show that the CO_2 and air flow sensor seems to be correct. As well CO_2 and air flow sensor faults are present once or twice. We ignore these outliers. The damper is diagnosed true because only one outlier was present, see Fig. 7.1(5).

The diagnosis results for the other faults shown in Figs. 7.1 (1), (3), (6), (8) and (9) indicate that in 2015 the next faults were present:

- *Occupancy*
- *AHU*
- *Window control*
- *BMS*
- *CO_2 control*

In Fig. 7.1(1) we see that the occupancy of the room is too high. Fig. 7.1(3) shows AHU faults and in Fig. 7.1(6) depicts that one or more of the windows are opened in some periods. Sometimes the data connection to the BMS is missing (see Fig. 7.1 (8)). From Fig. 7.1(9) we see that the CO_2 control is not working correctly sometimes.

In the next section the diagnosis results are discussed and validated with measured data and from facility manager information.

8. Evaluation of the diagnosis results

8.1 Findings from users and facility management

Occupancy information and information from the technical facility manager are used to analyze the diagnosis results. Below the findings are presented.

Fault 1: *Occupancy*

Room 1.067 is an office room for lecturers which was designed for an occupancy of 4 persons (800 ppm at a fresh air ventilation rate of 200 m3/h with an outdoor CO_2 concentration of 400 ppm). However 6 workplaces are present in room 1.067 which, according to lecturers, are regularly fully occupied sometimes, so the room can be fully occupied especially in the busy education periods of June and September leading to higher occupancy than by design rules. Thus signalized occupancy faults seem to be reasonably reliable.

Fault 3: *AHU*

AHU faults were estimated by diagnosis at the begin of January. It was known from the facility manager of THUAS that the supply fan in the AHU was off by malfunction of the AHU control from 6th till 12th January 2015 because this fan was set off automatically by a control rule to protect freezing of the AHU heater. However, it was not reset just in time but a few days later. Additionally, for some reasons, probably wrong signal connection with the BMS, the fan stayed off while ventilation was needed during 49 hours in year 2015. But we saw that after some hours the fan was set on and the fault was, probably automatically, restored. Thus, this fault was right diagnosed all the time.

Fault 6: *Window control*

The registered time that windows are opened and the CO_2 concentration is higher than 800 ppm, is 58 hours. The BMS data contains also changes of the values of the contacts which registries opened windows. We have ignored consciously this data for diagnosis purposes which makes it possible to validate diagnosis outcomes concerning window control. Looking at this original BMS data, showed that one or both windows were opened during that hours. Thus the diagnosis delivered correct results.

Faults 8: *BMS*

From the log book at the facility manager is was known that sometimes the data connection between the BMS and the data storage was broken.

Faults 9: *CO2 control*

There were complaints, but nothing was done about it, because facility management thought it would come from the windows.

8.2 Conclusions from the case study

The case study shows the usefulness of the proposed 4S3F method for a DCV system. In almost all cases the diagnosis is correct. Only 4 outliers, one for the CO_2 sensor, one for the room damper and two for the qV sensor were present. However, most of these false diagnoses can be prevented by using actual BMS data instead of hourly data based on a snapshot during a hour. Also, corresponding rules can be adapted. For instance by taken into account the diagnosis results of the hours before or after the hour that the diagnosis takes place, or by changing the thresholds values in the rules. The faulty diagnosis could be corrected when another rule is introduced to estimate symptom k, for instance considering a whole day.

We have not adapted rules and thresholds in the case study because it was not our intention to optimize rules and thresholds in this article.

9. Sensitivity analysis of the set probabilities

[34] states that the absolute values for as the prior and the conditional probabilities are not important but their relative values. A sensitivity analysis has been conducted on the DBN model presented in Fig. 4.2 to investigate this statement.

9.1 Change of set probabilities of faults at an isolated symptom

First, we consider the effect of variable set probabilities when a symptom and its linked faults are isolated from the other DBN nodes. As example we have analysed symptom *High CO2 and low qV* which DBN model is presented in Fig. B.1. In the case study the prior probabilities of *Damper* and *CO2 control* are set to 99 and 95 %. In addition the conditional true probabilities in the symptom node are set to 34 % and 90 % for a false *damper* and false *CO2 control*. When the symptom *High CO2 and low qV* is set to be true, The DBN calculated that the posterior false probabilities of *Damper* and *CO2 control* are 8 and 93 %. Fig. 9.1 to 9.4 present the results of a sensitivity analysis on prior and conditional probabilities. In Fig. 9.1 the diagnosed posterior false probabilities of the faults are presented as function from the prior false probability of *Damper*. As can be seen, the posterior false P(*Damper*)'s are still higher than those of *Window control* when its prior value is changed from the assumed 1 % in Table B.2 to 10 %.

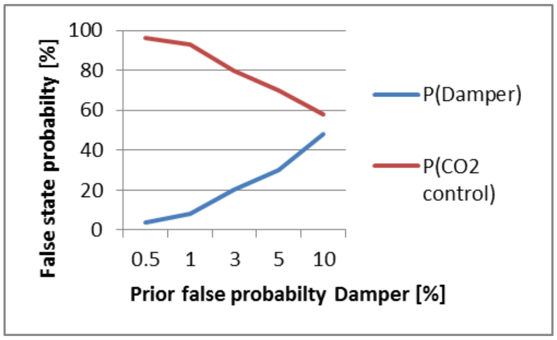

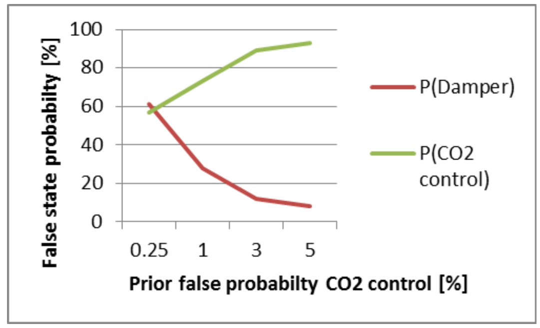

Fig. 9.1 Effects prior probability *Damper*

Fig. 9.2 Effects prior probabilities *CO2 control*

In the same way, we see that adapting of the prior probability of the *CO2 control* from 0.5 to 5 % does not lead to other trends in fault identification. Fig. 5.3 and 5.4 show the effects of changes of conditional probabilities. In a wide range of conditional probabilities the outcome trends are the same.

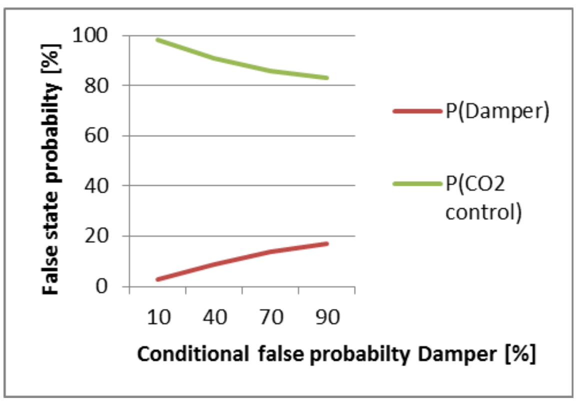

Fig. 9.3 Effects conditional probability *Damper*

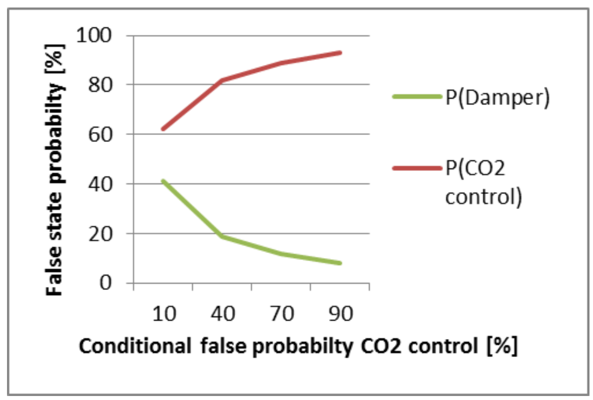

Fig. 9.4 Effects conditional probabilities *CO2 control*

9.2 Change of set probabilities of faults on the diagnosis results

Here, we present the diagnosis results of the case study when some of the set probabilities concerning symptom *high CO2 and no qV*, see the isolated DBN model in Fig. 9.5, are changed arbitrary in such way that the differences with the probabilities of other nodes decrease.

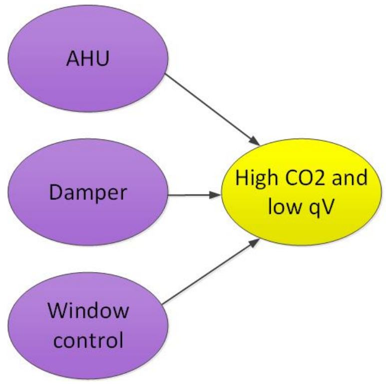

Fig. 9.5 DBN model for symptom *high CO2 and no qV*.

The next changes are made:

- Prior false probability of *AHU* is set to 2 instead of 1 %.
- Prior false probability of *Window control* is set to 2 instead of 5 %.
- Conditional false probability of *AHU* in *High CO2 and qV=0* is set to 90 instead of 70 %.
- Conditional false probability of *Window control* in *High CO2 and qV=0* is set to 20 instead of 40 % .

Fig. 9.6 shows the differences between the estimated posterior fault probabilities and the results shown in Fig. 8.1.

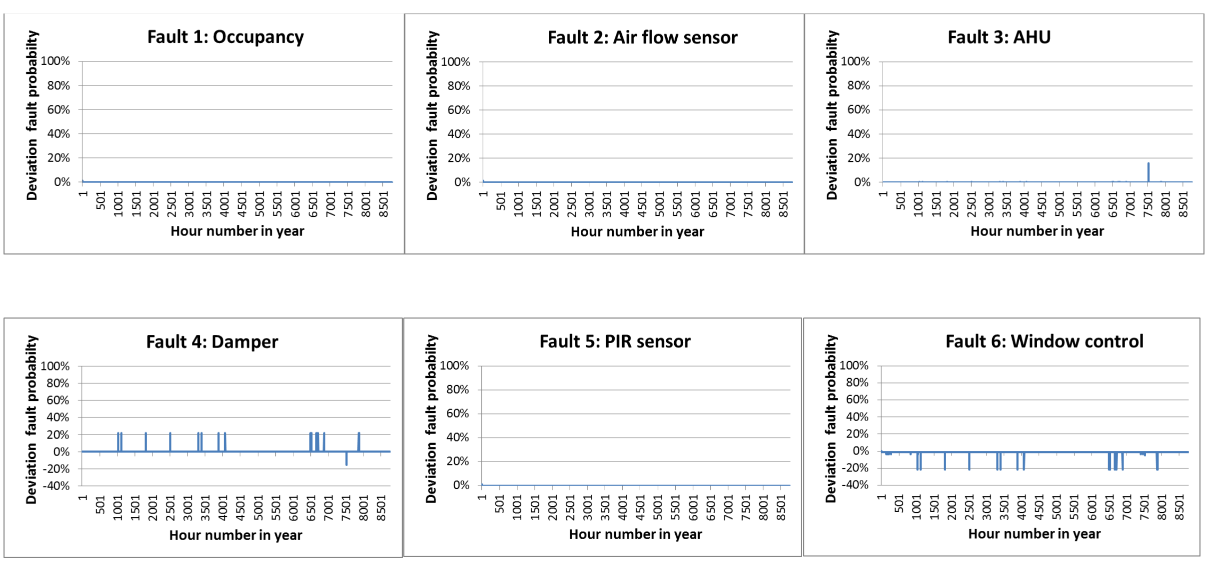

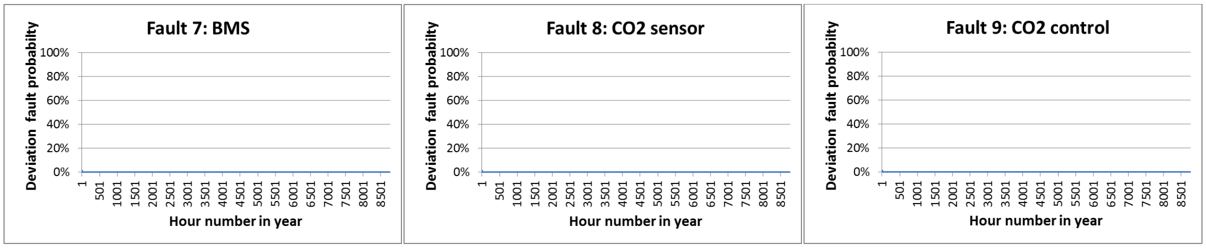

Fig. 9.6 Diagnosis deviation by different set prior and conditional probabilities related to symptom *High CO_2 and $qV=0$*.

As can be seen, one outlier is present for *AHU*. Furthermore *Damper* and *Window control* show deviations. However, even when the posterior fault probabilities presented in section 8 are corrected for these deviations they stay higher than 30 % to take action for correction as noted in section 4. This can be seen from Fig. 9.7 in which for faults 3, 4 and 6 the posterior fault probabilities are shown in blue and the deviations in red.

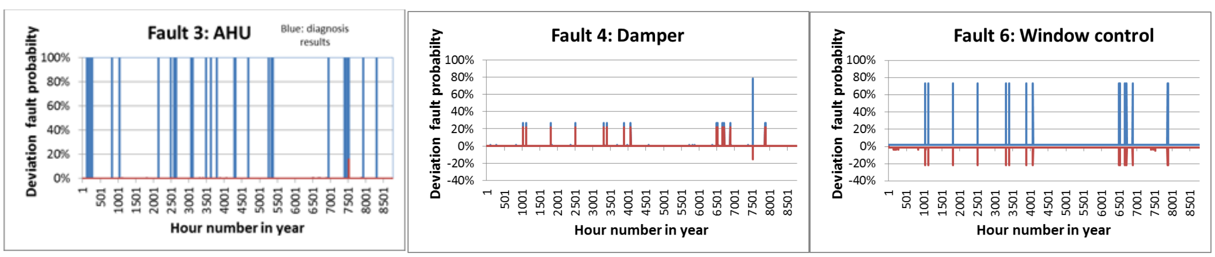

Fig. 9.7 Effects on posterior probabilities at changed set probabilities to symptom *High CO_2 and $qV=0$* (red: deviation after changed set, blue: diagnosis results)

The sensitivity analyses show that variation in set prior and conditional probabilities did not lead to other diagnosis outcomes which confirms our statement that absolute values are of secondary importance. Detailed historical data on probabilities of the states is therefore not necessary, thus no detailed training data, but expertise about the relative frequency of errors occurring which is known by design and maintenance HVAC engineers. Also component knowledge can be taken into account.

10. Conclusions and recommendations

Conclusions

In this article the 4S3F FDD method for Energy Performance diagnosis has been applied on a DCV system. A generic set of symptoms and faults has been proposed and a case study has been conducted on the DCV system in a school building for the year 2015. This case study shows the usefulness of the proposed FDD method. In most cases the diagnosis seems correct despite arbitrary assumptions in symptom rules and for the probability values in de DBN model. Only 4 faulty diagnosis outliers were noted.

The DCV 4S3F method can be implemented simultaneously with the BMS system which are both based on HVAC P&IDs, like showed in Fig. 3.1, as applied at HVAC design. Symptom rules and their thresholds depend on the specific DCV system. However, they can be estimated by the HVAC designer. Detection and diagnosis models could be obtained from libraries because of the generic approach in the 4S3F method. In addition DCV faults are generic because of the generic character of the components and controls.

The sensitivity analyses in section 9 show that even when the set prior and conditional probabilities are varied in a wide range, this do not lead to other diagnosis outcomes as long as their relative values show the same trends as in reality.

Recommendations

Below recommendations are presented for improvement of the DCV FDD method.

Actual BMS data

In the case study hourly historical BMS data is used. The diagnosis can be proved applying real time actual BMS data. There is no limitation in the 4S3F method to use shorter periods. However some rules have to be adapted to transient behaviour of the HVAC system and measurements outliers.

Extension with control signals from controllers

In practice, more actual BMS data is available like state and control values of actuators and controllers. The presented end-terminal system can be extended by these parameters to distinguish control and component faults of the damper and the supply fan.

Extension with AHU components

In the case study all faults in AHU are combined to one fault. One could distinguish damper, filter, fan and control faults to isolate the fault more precisely.

Recommendation to estimate and correct biased CO_2 sensors

Biased CO_2 sensors can be estimated faster and more accurately by implementing additional fully mechanical ventilation of each room during night time. In this way a deviation in the CO_2 measurement can be estimated with the help of a mass balance symptom.

Counting persons

A simple method to count or calculate the number of persons in a room is helpful to estimate too high occupancy. This virtual sensor can be based on the increase of the CO_2 concentration and the supplied air flow. See e.g. Timilehin et al. [35] who presented an occupancy measurement survey.

Extension with specific FDD methods for components

As stated for the EP FDD, the FDD method for DCV systems can be extended with existing and new FDD methods for components as additional symptoms.

Extending the DCV FDD to VAV FDD

The proposed DCV FDD can be extended to VAV FDD by taking into account heat exchangers in the end terminals and thermal comfort control. In this way, thermal comfort indicators like air and wall temperatures and humidity can be integrated.

Optimizing the symptom rules

In the case study values in symptom rules are set up arbitrary and further studies are needed to determine optimal setpoints.

Setup of model libraries

We propose to set up model libraries for standard components and symptom rules.

- Symptom rules with default thresholds.
- DBN models including default prior and conditional probabilities for the fault and symptom nodes.

Automation of prior and conditional probabilities

As noted during the sensitivity analyses, the absolute values of the set probabilities are not very sensitive for the diagnosis results but the relative values are. We propose to do research for automation of the set probabilities based on ranking of probabilities by HVAC expertise or by applying machine learning.

Integrating the DCV FDD with energy performance (EP) FDD

Misfunction of DCV systems leads to poor indoor climate but also to energy waste. Coupling the 4S3F method for energy performance diagnosis and Energy and the DCV 4S3F method gives the possibility for redundancy and therefore more accurate energy performance diagnosis.

Appendix A Symptoms and faults of a DCV system

A symptom is an entity that can be observed directly and automatically from the sensors installed in the system. Finding all possible symptoms is just a matter of looking at all measurement points and analyzing what can be known from them. On the contrary, faults are anything that can go wrong. Symptoms and faults are derived from the observation of the P&ID in Fig. 3.1 and summarized in Table A.1.

SYMPTOMS	
Code	Balance symptoms
S1 S2 S3	- Deviations in CO2 mass balances (e.g. the supplied CO2 mass must be equal to the discharged CO2 mass plus the increase of the CO2 mass) - Deviations in air mass balances (e.g. by air flow rate sensor fault) - Deviations in pressure balances (e.g. by air leakage which effects the supplied air rate.)
	Operational state (OS) symptoms
S4 S5 S6 S7 S8 S9	- The measured CO_2-concentration by CT is higher than the setpoint C_{sp}. - Unexpected low or high CO_2 concentration. - Unexpected low or high air flows. - Missing BMS data - Unrealistic sensor data - Presence outside working hours
	Additional symptoms
S10 S11 S12 S13	- Maintenance information - Information from inspection. - Sensor calibration information - Complaints from occupants.
FAULTS	
Code	Model faults
F1 F2	- Model faults for virtual sensors, a physical missing state value is calculated by software from existing sensors, to estimate for instance presence and occupancy. E.g. by CO_2 increase one could estimate the number of occupants in a room. - Assumptions to set up CO_2- and air balances in the rooms.
	Component faults
F3 F4 F5	- Supply fan or return fan, including electromotor, in the Air Handling Unit (AHU) is not working properly or broken. - One of the dampers (also including electromotor) at the AHU is not working properly or broken.

F6	- Inlet filter of the AHU is polluted which lead to low air flow to the building.
F7	- Leakage of ducts or clogged ducts.
F8	- Room damper (in which the motor is included) is broken.
F9	- CO_2 sensor is defective or biased.
F10	- Presence sensor is defective or biased.
F11	- Window contact sensor is defective or biased.
F12	- Flow rate sensor is defective or biased.
F13	- Data connection from the room sensors to the BMS is missing.
F14	- Data connection to the BMS is missing.
	- Data connection to the dampers of the AHU is broken.
	Control faults
F15	- Control of the supply and return fan by controller PC is faulty
F16	- Control of the CO_2 concentration by controller CC is faulty.
F17	- Control of the AHU dampers by controller VC is faulty.
F18	- Room occupancy is higher than designed.
F19	- Windows are opened while mechanical ventilation is needed.

Table A.1 Faults and symptoms related to the DCV system of Fig. 3.1.

Faults F18 by over occupancy and F19 by window control are noted as control faults because people are not using the room or controlling the system as it was intended. In the first case, may be facility management allowed more persons in the room than allowed by design. The second because the occupants in the room let the windows too long opened which results in missing mechanical ventilation. A BMS fault could be a broken wiring or a software fault by failure of the communication application which lead to missing data. So it is categorized as a component fault.

Appendix B The construction of the 4S3F DBN

We consider a small part from the DCV DBN model of Fig. 4.2 to show how the DBN calculates fault probabilities. Symptom *High CO2 and low qV* is taken into account. From Fig. 4.2 we see that this symptom can be caused by a faulty *CO2 control* or faulty *Damper*. The faults linked to this symptom (notice that arcs go from the fault node to the symptom node) are isolated from other symptoms in this example which results in the DBN model shown in Fig. B.1.

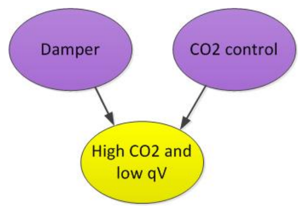

Fig. B.1 DBN model for symptom *High CO2 and low qV*.

Faults are parent nodes with prior probabilities. We define the probability as the number of presence per 100 observations divided by 100.

The prior true probability that the damper (P(Damper)) is correct, has an arbitrary value of 99 % (see Table B.1) and the prior true probability P(CO2 control) is set lower to 95 % (see Table B.2) because from experience it is known that control faults occurs often than component faults. These values can be adapted by historical values from the BMS and inspection of the log book at the facility manager or by complaints from occupants.

'Damper' state	***Probability***
False	*0.01*
True	*0.99*

Table B.1 Prior properties *Damper*.

'CO2 control' state	***Probability***
False	*0.05*
True	*0.95*

Table B.2 Prior properties *CO2 control*.

In Genie [36], a DBN software tool, this can be implemented in tables for the node properties as shown in Tables B.1 and B.2. Symptoms are child nodes with conditional probabilities depending on the state of the fault node. Table B.3 presents possible node properties for symptom *High CO2 and low qV* where a true value for the symptom indicates that the symptom is present. For the sake of simplification it is assumed in this example that when one of the faults is present, the symptom is also present.

Damper	**False** (0.01)		**True** (0.99)	
CO2 control	**False** (0.05)	**True** (0.95)	**False** (0.05)	**True** (0.95)
High CO2 and low qV: True (symptom is present)	1	1	1	0
False	0	0	0	1

Table B.3 Conditional node properties *High CO2 and low qV*

(between parentheses: the prior probabilities).

As can be seen symptom *High CO2 and low qV* is present when *Damper* or *CO2 control* is false, otherwise true because as well *Damper* and *CO2 control* is true. In this example we can easily calculate the probability that *High CO2 and low qV* is false (P(*High CO2 and low qV*)=0), thus no symptom is present, when both faults are not present because faults *Damper* and *CO2 control* are statically independent of each other:

P(*High* CO_2 *and low qV*)= P(*Damper* ∧CO_2 *control*)=P(*Damper*).P(CO_2 *control*)= 0.99*0.95=0.9405=94.05 %. In Table B.4 all calculated symptom probabilities are shown.

Damper	**False** (0.01)		**True** (0.99)	
CO2 control	**False** (0.05)	**True** (0.95)	**False** (0.05)	**True** (0.95)
True	0.05 %	0.95 %	4.95 %	0
False	0	0	0	94.05 %

Table B.4 Calculated probabilities *High* CO_2 *and low qV* from the fault states.

Conversely, it is possible to calculate the fault probabilities P(*Damper*) and P(CO_2 *control*) when the state of symptom *High* CO_2 *and low qV* is known. For instance the posterior fault probability of *Damper* can be calculated from (0.05+0.95)/(0.05+0.95+4.95)=0.168=16.8 % when symptom *High* CO_2 *and low qV* is detected. Note that the posterior fault probabilities are estimated in the DBN from symptoms to faults while the DBN is set up from faults to symptoms. In Figs. B.2 and B.3 two examples are presented for symptom *High* CO_2 *and low qV*. Fig. B.2 shows the estimated symptom probabilities (94.1 % false) with the prior fault probabilities and Fig. B.3 presents the estimated posterior fault probabilities when a symptom is detected (see that the *Damper* posterior false probability is 16.8 % as mentioned earlier).

In Genie the type of the child nodes can be selected. In the general type, the child nodes have probabilities for each combination of parent states. Most of the time it is impossible or time consuming to define the fault probabilities of all these combinations.

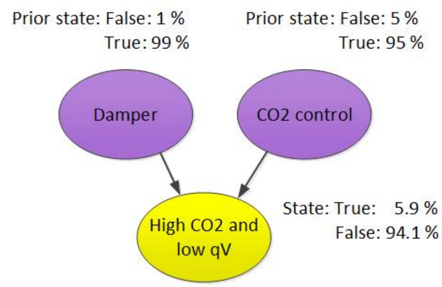

Fig. B.2 Estimation of symptom probabilities (takes place during the setup of the DBN)

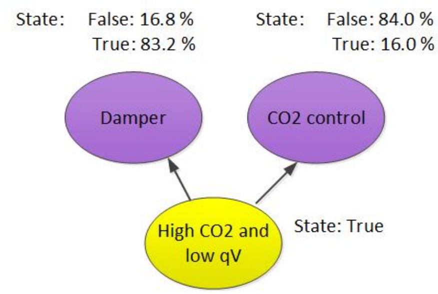

Fig. B.3 Estimation of fault probabilities (takes place automatically place by DBN during FDD process

In the 4S3F method we apply so-called Noisy-Max nodes in which the false parent state indicates the chances of the child states. Table B.5 presents this for our DBN example. *High CO2 and low qV* can be 66 % false (symptom not present) when *Damper* is false or 10 % false when *CO2 control* is false. The conditional false probability by a false *Damper* is high because a frozen damper can be closed or largely opened which does not result in a small air flow rate. LEAK shows here the chance of the state properties when *Damper* and *CO2 control* are both true. Adjustment of the DBN example with the Noisy-Max node presented in Table B.3 leads both to 1 % false values for *Damper* and *CO2 control* when *High CO2 and low qV* is false, while the false values are 7.7 and 93.3 % when *High CO2 and low qV* is true.

State symptom 'High CO2 and low qV'	***Damper False***	***CO2 control False***	***LEAK***
True (symptom detected)	*0.34*	*0.90*	*0*
False (symptom not detected)	*0.66*	*0.10*	*1*

Table B.5 Noisy-Max type for node *High CO2 and low qV* in the DBN example

Noisy-Max nodes were applied for all DCV symptom nodes. The fault nodes, see Tables B.1 and B.2, have as first state the false state because it is difficult to estimate the probabilities of the child node when one of the parent nodes is true independent of the state of the other parent nodes. In this way the Noisy-Max probabilities can be set up easily because the true state of LEAK can be set to 1 as we assume that the symptom is not detected when both faults are not present. Only an inaccurate model to detect symptoms could lead to a detected symptom while actually no faults are present. We have ignored this option.

As shown in Tables B.1, B.2 to B.5, only false and true states are proposed for the fault and symptom nodes in the DCV DBN. However it can be extended with more states when necessary.

References

[1] W. Fisk, A. de Almeida, 1998. Sensor-based demand-controlled ventilation: a review. Energy and Buildings 29, 35–45.

[2] ASHRAE Standard 62.1-2013, Ventilation for Acceptable Indoor Air Quality; American Society of Heating, Refrigeration, and Air-Conditioning Engineers, Inc. Atlanta, GA, USA, 2013.

[3] A. Tukur, K. Hallihan, K. Kissock, Energy Savings from Robust Control of Static Pressure Based upon Zonal Occupancy for Multiple-Zone VAV Systems. Proceedings ACEEE Summer Study on Energy Efficiency in Buildings 2016.

[4] T. Nielsen, C. Drivsholm. Energy efficient demand controlled ventilation in single family houses Energy and Buildings, 42 (2010) 1995–1998.

[5] L. Schibuola, M. Scarpa, C. Tambani, Annual performance monitoring of a demand controlled ventilation system in a university library, Energy Procedia 101 (2016) 313-320.

[6] J. Zhang, G Liu, R. Lutes, M. Brambley. Energy Savings for Occupancy-Based Control (OBC) of Variable- Air-Volume (VAV) Systems. PNNL-22072. Pacific Northwest National Laboratory. 2013.

[7] J. Qin, S. Wang. A fault detection and diagnosis strategy of VAV air-conditioning systems for improved energy and control performances. Energy and Buildings 37 (2005) 1035-1048.

[8] S. Lee, F. Yik. A study on the energy penalty of various air-side system faults in buildings, Energy and Buildings 42 (2010) 2–10.

[9] Y. Guo, J. Wall, J. Li, S. West, Intelligent Model Based Fault Detection and Diagnosis for HVAC System Using Statistical Machine Learning Methods, ASHRAE Transactions. 2013, Vol. 119 Issue 1, Special section p1-8.

[10] Y. Yu, D. Woradechjumroen, D. Yu, A review of fault detection and diagnosis methodologies on air-handling units, Energy and Buildings 82 (2014) 550-262. dx.doi.org/10.1016/j.enbuild.2014.06.042

[11] S. Wang, Q. Zhou, F. Xiao, A system-level fault detection and diagnosis strategy for HVAC systems involving sensor faults, Energy and Buildings 42 (2010) 477–490.

[12] G. Okochi, Y. Yao, A review of recent developments and technological advancements of variable-air-volume (VAV) air-conditioning systems, Renewable and sustainable Energy Reviews 59 (2016) 784-817.

[13] K. Shan, Y. Sun, S. Wang, C. Yan. Development and in-situ validation of a multi-zone demand-controlled ventilation strategy using a limited number of sensors. Building and Environment 57 (2012) 28-37.

[14] B. Chenari, J. Carrilho, M. da Silva, Towards sustainable, energy-efficient and healthy ventilation strategies in buildings: A review, Renewable and Sustainable Energy Reviews 59 (2016), 1426-1447.

[15] T. Lu, X. Lü, M. Viljanen, A novel and dynamic demand-controlled ventilation strategy for CO2 control and energy savings in buildings. Energy and Buildings 43 (2011) 2499-2508.

[16] S. Goyal, H. Ingley, P. Barooah, Occupancy-based zone-climate control for energy-efficient buildings: complexity vs. performance, Applied Energy 106 (2013) 209-221.

[17] C. Chao, J. Hu. Development of a dual-mode demand control ventilation strategy for indoor air quality control and energy saving Building Environ, 39 (2004) 385–397.

[18] S. Wang, X. Xu, 2002. A Robust Control Strategy of Combined DCV and Economizer Control for Air-conditioning Systems. Energy Conversion and management, 43(18):2569-2588.

[19] W. Kim, S. Katipamula (2017). A Review of Fault Detection and Diagnostics Methods for Building Systems. Science and Technology for the Built Environment 24:1 3-21.

[20] H. Wang, Y. Chen, C. Chan, J. Qin, A Robust Fault Detection and Diagnosis Strategy for Pressure-independent VAV Terminals of Real Office Buildings, Energy and Buildings 43 (2011) 1774-1783.

[21] J. Seem, J. House, R. Monroe. On-line monitoring and fault detection. ASHRAE 1999:21-26.

[22] J. Schein, J. House. Application of control chart for detecting faults in variable-air-volume box. ASHRAE Trans 2003; 109(2): 671-82.

[23] A. Dexter and M. Benourats. A generic approach to identify faults in HVAC plants. ASHRAE Trans 1996;102 (1):550-556.

[24] H. Wang, Y. Chen, C. Chan, J. Qin, An online fault diagnosis tool of VAV terminals for building management and control systems, Automation in Construction 22 (2012) 203-211.

[25] Z. Du, X. Jin. PCA-FDA-based fault diagnosis in VAV systems. HVACRes 2007;13(2):349–67.

[26] H. Qi, W. Dong, A FDD model of VAV systems based on neural-networks and residual statistics. Proceedings from 14th international conference on control, automation, robotics and vision, Phuket Thailand, 13-15th November 2016 (ICARCV 2016). 1555-1559.

[27] F. Xiao, Y. Zhao, J. Wen, S. Wang, Bayesian network based FDD strategy for variable air volume terminals. Automation in Construction 41 (2014): 106-118. https://doi.org/10.1016/j.autcon.2013.10.019.

[28] A. Regnier, J. Wen, Automated Fault Diagnostics for AHU-VAV Systems: A Bayesian Network Approach. International High Performance Buildings Conference. July 2018. Paper 235. https://docs.lib.purdue.edu/ihpbc/235.

[29] Y. Zhao, J.Wen , F. Xiao, X. Yang, S. Wang, Diagnostic Bayesian networks for diagnosing air handling units faults – part I: Faults in dampers, fans, filters and sensors. *Applied Thermal Engineering* 111 (2017): 1272-1286.

[30] Y. Zhao, J. Wen, S. Wang, 'Diagnostic Bayesian networks for diagnosing air handling units faults – Part II: Faults in coils and sensors,' *Applied Thermal Engineering* 90 (2015): 145-157. https://doi.org/10.1016/j.applthermaleng.2015.07.001.

[31] Y. Zhao, S. Wang. An intelligent chiller fault detection and diagnosis methodology using Bayesian belief network. Energy and Buildings 57 (2013) 278–288.

[32] K. Verbert, R. Babuska, B. De Schutter. Combining knowledge and historical data for system-level fault diagnosis of HVAC systems. Engineering Applications of Artificial Intelligence 59 (2017) 260-273.

[33] J. Chen, J. Wen, T. Chen, O. Pradhan, Bayesian Networks for whole building level fault diagnosis and isolation. International High Performance Buildings Conference. July 2018. Paper 266. https://docs.lib.purdue.edu/ihpbc/266.

[34] A. Taal, L. Itard, W. Zeiler. (2018), A reference architecture for the integration of automated energy performance fault diagnosis into HVAC systems. Energy & Buildings 179, 144-155.

[35] L. Timilehin, W. Zeiler, Z. Yang, Occupancy measurement in commercial office buildings for demand-driven control applications, A survey and detection system evaluation, Energy and buildings (2015).

[36] GeNie 2.1, BayesFusion. http://download.bayesfusion.com, 2019 [accessed 16.05.19].